Supporting Text

This supporting text is split into the following three sections

1. Description of simplified models.
2. Justification of parameter constraints.
3. Supplementary results and proofs (Results S1–S13).

The first section describes the derivation of a set of simplified models (A–C), which are used to generate analytic expressions concerning robustness (Equations (9)–(17), main text). The second section describes and justifies a number of constraints (C1–C10) that were used in estimating parameter from existing experimental data. The final section provides mathematical proofs that complement the results in the first two sections and in the main text.

1 Description of simplified models

In order to analyse specific aspects of the full model, and to facilitate parameter estimation, we introduce three simplified models that focus on different aspects of gradient formation. Model A is a simple free diffusion model for Hedgehog movement, neglecting any effects of HSPGs. Model B simplifies the anterior compartment equations, so that the anterior gradient can be approximated as an exponential. To focus on feedbacks and regulation within the signalling pathway, Model C is a simplified model of the Hedgehog gradient in the anterior compartment. As can be seen in the figure below (Fig. ST1), Models B and C provide reasonable approximations to the full model.

Using these models, we can obtain approximations for the steady-state Hedgehog gradient in the full model, and for a number of quantities of relevance for our investigation of robustness, including α_0 (Eqns. (9) and (10)), x_P (Eqn. (11)), α_A (Eqn. (13)), x_A (Eqn. (14)), g (Eqn. (15)) and β (Eqns. (16) and (17)).

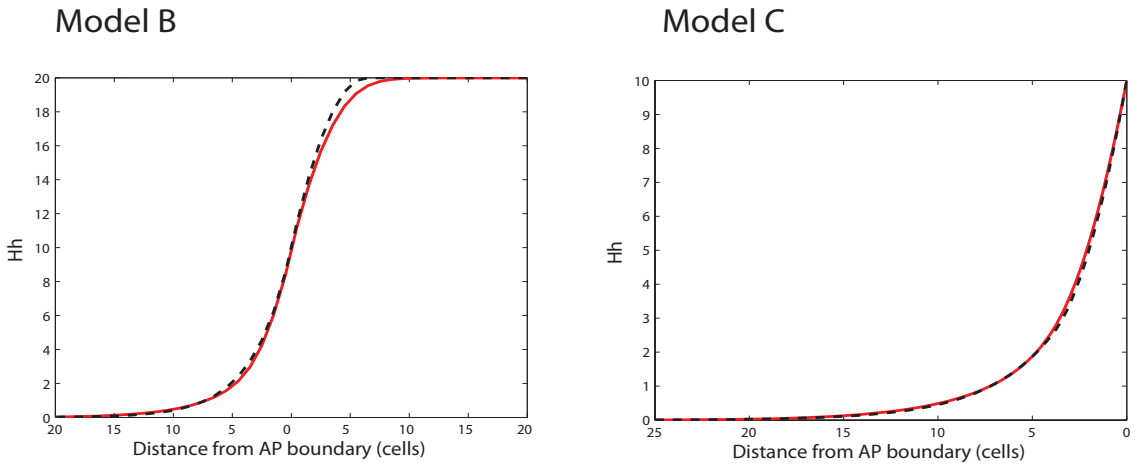

Figure ST1: Steady state HH gradients in Models B and C (dashed line) compared to that in the full model (red line). $\gamma(A) = 0.75k_{on}$ and $\delta k_{on} = 0.6k_{on}$, respectively. The remaining parameters are listed in Table 1 of main text.

Model A: Simplified free diffusion model

To address the role of regulated diffusion in the full model, we introduce a free diffusion model for Hedgehog gradient formation (for comparison with regulated diffusion models). As in the full model we represent the disc as a one dimensional cross section $-L_A \leq x \leq L_P$, with distinct equations for the posterior and anterior compartments:

$$\frac{\partial [HH_b]}{\partial t} = \begin{cases} \rho_h + D_b(P)\dfrac{\partial^2 [HH_b]}{\partial x^2} - \gamma(P)[HH_b], & 0 \leq x \leq L_P \text{ (posterior)}, \\ \\ D_b(A)\dfrac{\partial^2 [HH_b]}{\partial x^2} - \gamma(A)[HH_b], & -L_A \leq x < 0 \text{ (anterior)}. \end{cases}$$

In this model, we assume that Hedgehog is produced only in the posterior compartment, but that it can diffuse and is degraded in both compartments. There are no effects of HSPGs on Hedgehog movement or stability. However, for generality, we allow diffusion and degradation rates (D_b and γ respectively) to vary between the posterior and anterior compartments.

The steady state solutions (setting $\dfrac{\partial [HH_b]}{\partial t} = 0$) are given by

$$[HH_b] = \begin{cases} \dfrac{\rho_h}{\gamma(P)} + a\cosh\left(\dfrac{x}{\lambda_P}\right) + b\sinh\left(\dfrac{x}{\lambda_P}\right), & 0 \leq x \leq L_P \text{ (posterior)}, \\ \\ c\exp\left(\dfrac{x}{\lambda_A}\right) + d\exp\left(\dfrac{-x}{\lambda_A}\right), & -L_A \leq x < 0 \text{ (anterior)}, \end{cases}$$

for arbitrary constants a, b, c and d, where $\lambda_i = \sqrt{\frac{D_b(i)}{\gamma(i)}}$. Assuming zero flux boundary conditions at $x = -L_A$ and $x = L_P$, we obtain

(i) $b = -a \tanh\left(\frac{L_P}{\lambda_P}\right)$,

(ii) $d = c \exp\left(\frac{-2L_A}{\lambda_A}\right)$.

Assuming $L_A \gg \lambda_A$, then (ii) implies that $d \ll c$, and so we can approximate $d = 0$ and treat the anterior compartment gradient as a pure exponential decay.

By matching $[HH_b]$ at $x = 0$, we obtain

(iii) $a = c - \frac{\rho_h}{\gamma_b(P)}$

Although unequal diffusion rates ($D_b(P) \neq D_b(A)$) can lead to discontinuity at the AP boundary, the magnitudes of the posterior gradient (g_P) and anterior gradient (g_A) at the AP boundary are still related by $D_b(P)g_P = D_b(A)g_A$ (Result S1 in Section 3 of this *Supporting Text*). This then leads to

(iv) $b = c\frac{D_b(A)}{D_b(P)}\frac{\lambda_P}{\lambda_A}$

Solving in terms of $c = \alpha_0$ ($[HH_b]$ at $x = 0$), then gives

$$\alpha_0 = \frac{\rho_h}{\gamma(P)}\left(\frac{\tanh\left(\frac{L_P}{\lambda_P}\right)}{\frac{D_b(A)}{D_b(P)}\frac{\lambda_P}{\lambda_A} + \tanh\left(\frac{L_P}{\lambda_P}\right)}\right). \qquad \text{(Giving Eqn 9)}$$

Solutions for a, b and d then follow. Moreover, as proved in Result S2 (in Section 3 of this *Supporting Text*), the ratio between Hedgehog levels at the posterior margin ($x = L_P$) and the AP border ($x = 0$) is given by

$$\beta = 1 + \frac{D_b(A)}{D_b(P)}\frac{\lambda_P}{\lambda_A}\left(\frac{1}{\tanh\frac{L_P}{\lambda_P}}\left(1 - \frac{1}{\cosh\frac{L_P}{\lambda_P}}\right)\right). \qquad \text{(Giving Eqn 16)}$$

Model B: Simplified regulated transport model

To approximate the steady-state HH gradient for the full model, and to analyse further the role of regulated transport, we focus on $[HH_b]$ and split the posterior compartment into two distinct regions. We assume that HSPGs become saturated with HH in the posterior-most region of the disc (i.e. for $x_P < x \leq L_P$). In this region, $[HH_b] = \mu$, where μ is the carrying capacity of HSPGs. In the remainder of the disc, Hedgehog gradient formation is described by the following equations:

$$\frac{\partial [HH_b]}{\partial t} = \begin{cases} \rho_h + D_b(P)\dfrac{\partial^2 [HH_b]}{\partial x^2}, & 0 \leq x \leq x_P \text{ (posterior)}, \\ \\ D_b(A)\dfrac{\partial^2 [HH_b]}{\partial x^2} - \gamma(A)[HH_b], & -L_A \leq x < 0 \text{ (anterior)}. \end{cases}$$

The regulation of HH transport and stability are incorporated via the parameters μ, D_b and γ_b in the full model. HSPGs can modulate HH transport through the parameter D_b. For simplicity, we assume that this rate is constant within each compartment but may differ between posterior and anterior compartments ($D_b(P)$ vs $D_b(A)$). Stabilisation of HH by HSPGs is incorporated in the parameter γ_b (by assuming that γ_b is small).

We derive an approximate equation for HH for $x \in [0, x_P]$ as follows. In the full model (Eqns. (1) and (2), main text), assume that D_f, k_{in} and γ_b are relatively small. Setting $[HH_f]$ to steady state ($\dfrac{\partial [HH_f]}{\partial t} = 0$) then gives

$$\frac{\partial [HH_b]}{\partial t} \approx \frac{\rho_h k_{out}(\mu - [HH_b])}{\gamma_f + k_{out}(\mu - [HH_b])} + D_b(P)\frac{\partial^2 [HH_b]}{\partial x^2}.$$

By assuming that k_{out} is sufficiently large, we arrive at the approximate equation for $[HH_b]$ for $x \in [0, x_P]$. As for model A, we approximate the dynamics of HH in the anterior compartment as a simple diffusion-degradation system, giving an approximately exponential gradient.

Assuming L_A and $\gamma(A)$ are sufficiently large to ensure that an exponential approximation for the anterior gradient is appropriate, we obtain the following steady state solutions for $[HH_b]$:

$$[HH_b] = \begin{cases} \mu, & x_P < x \leq L_P \text{ (posterior)}, \\ \\ -\dfrac{\rho_h}{2D_b(P)}x^2 + bx + c, & 0 \leq x \leq x_P \text{ (posterior)}, \\ \\ d\exp\left(\dfrac{x}{\lambda_A}\right), & -L_A \leq x < 0 \text{ (anterior)}, \end{cases}$$

for arbitrary constants b, c and d and $\lambda_A = \sqrt{\dfrac{D_b(A)}{\gamma(A)}}$. Imposing continuity of the gradient and flux within the posterior compartment (and assuming $x_P < L_P$) gives

(i) $\frac{\rho_h}{2D_b(P)}x_P^2 - bx_P + (\mu - c) = 0,$

(ii) $b = \frac{\rho_h}{D_b(P)}x_P.$

Moreover, ensuring $[HH_b]$ is equal at $x = 0$, in both the anterior and posterior equations, we obtain

(iii) $c = d.$

Although unequal diffusion rates ($D_b(P) \neq D_b(A)$) can lead to discontinuity at the AP boundary ($x = 0$), the magnitude of the posterior gradient (g_P) and anterior gradient (g_A) at the AP boundary are related by $D_b(P)g_P = D_b(A)g_A$ (analogous to model A; Result S1). This then leads to

(iv) $d = b\lambda_A \frac{D_b(P)}{D_b(A)}.$

Substituting from conditions (ii)–(iv) into (i), and solving the quadratic, yields the following expression for $c = \alpha_0$ ($[HH_b]$ at $x = 0$):

$$\alpha_0 = \frac{\rho_h \lambda_A^2 D_b(P)}{D_b(A)^2}\left(-1 + \sqrt{1 + \frac{2\mu D_b(A)^2}{\rho_h \lambda_A^2 D_b(P)}}\right). \qquad \text{(Giving Eqn 10: } x_P < L_P\text{)}$$

The corresponding expression for x_P can then be calculated as

$$x_P = \lambda_A \frac{D_b(P)}{D_b(A)}\left(-1 + \sqrt{1 + \frac{2\mu D_b(A)^2}{\rho_h \lambda_A^2 D_b(P)}}\right). \qquad \text{(Giving Eqn 11)}$$

Moreover, as proved in Result S3 (in Section 3 of this *Supporting Text*), the ratio between HH levels at the posterior margin (μ) and the AP boundary (α_0) is given by

$$\beta = \frac{\mu}{\alpha_0} = \frac{1}{2} + \sqrt{\frac{1}{4} + \frac{\mu D_b(A)^2}{2\rho_h \lambda_A^2 D_b(P)}}. \qquad \text{(Giving Eqn 17)}$$

If $x_P \geq L_P$, then HSPGs do not become saturated with HH within the disc and model B is equivalent to model A with $\gamma(P) = 0$. As proved in Results S4 an S5 (in Section 3 of this *Supporting Text*), letting $\gamma(P) \to 0$ in model A results gives

$$\alpha_0 = \frac{\rho_h \lambda_A L_P}{D_b(A)}, \qquad \beta = 1 + \frac{L_P D_b(A)}{2\lambda_A D_b(P)}. \qquad \text{(Giving Eqn 10: } x_P > L_P\text{)}$$

Model C: Simplified anterior model

Since the Hedgehog signalling pathway is operative only in anterior compartment cells, we also introduce an approximate model that focuses on the Hedgehog gradient in anterior cells. Here, we consider the anterior compartment to be a one dimensional cross section $x \in [0, L_A]$ (for convenience, we take x to be positive here, as opposed to negative in the full model, when describing anterior distances).

We fix the level of $[HH_b]$ at the AP boundary to α_0 and then split the anterior compartment into two distinct regions by assuming that when HH levels are above a certain threshold ($[HH_b] > \alpha_A$; $x < x_A$), Patched is up-regulated at the highest rate $\rho_{p1} + \rho_{p2}$ (i.e. $f_p([S]) = 1$). The model equations for the two regions of the anterior compartment are then

$$\frac{\partial [HH_b]}{\partial t} = \begin{cases} D_b \dfrac{\partial^2 [HH_b]}{\partial x^2} - (\rho_{p1} + \rho_{p2}), & 0 \leq x < x_A, \\ \\ D_b \dfrac{\partial^2 [HH_b]}{\partial x^2} - k_{on} \delta [HH_b], & x_A \leq x \leq L_A. \end{cases}$$

To obtain the above approximation for $x \in [0, x_A)$ from the full model, we set $[PH]$ to steady state ($\dfrac{\partial [PH]}{\partial t} = 0$ in Eqn. (6)) to give

$$k_{on}[HH_b][PTC] - k_{off}[PH] = \gamma_{ph}[PH]$$

Then, assuming that $[HH_f]$, k_{in} and γ_b are relatively small, Eqn. (4) becomes

$$\frac{\partial [HH_b]}{\partial t} = D_b \frac{\partial^2 [HH_b]}{\partial x^2} - \gamma_{ph}[PH].$$

Then, using Result S8(c) (in Section 3 of this *Supporting Text*) and letting $f_p([S]) = 1$, this approximates to

$$\frac{\partial [HH_b]}{\partial t} = D_b \frac{\partial^2 [HH_b]}{\partial x^2} - (\rho_{p1} + \rho_{p2}) \left(\frac{\dfrac{\gamma_{ph} k_{on} [HH_b]}{k_{off} + \gamma_{ph}}}{\gamma_p + \dfrac{\gamma_{ph} k_{on} [HH_b]}{k_{off} + \gamma_{ph}}} \right).$$

Assuming $\gamma_p < k_{on}[HH_b]$ (which is necessary for a realistic gradient) and that k_{off} is relatively small yields the above approximation for $x \in [0, x_A)$.

As with models A and B, we approximate HH dynamics in the remainder of the anterior compartment ($x \geq x_A$) as a simple diffusion-degradation system, giving an approximately exponential gradient. Since the dominant process for removal of HH is binding to PTC at rate k_{on}, we represent degradation by the single term $k_{on}[HH_b][PTC]$ from the full model, approximating $[PTC]$

levels by a constant δ. As can be seen in Results S9 and S10 (in Section 3 of this *Supporting Text*), $\delta \equiv [PTC]$ levels in this region can be bound as follows (assuming k_{off} is relatively small)

$$\frac{z_A(\gamma_{ph} + r\rho_{p1})}{\gamma_{ph} + r\gamma_p z_A} \leq \delta \leq \frac{z_A(\gamma_{ph} + r(\rho_{p1} + \rho_{p2}))}{\gamma_{ph} + r\gamma_p z_A + k_{off}}, \qquad \text{(Eqn 18)}$$

where z_A is value of $[Z] = \dfrac{[PTC]}{1 + r[PH]}$ corresponding to the Patched production threshold (note that this value of z_A also corresponds to a unique value (s_A) of $[S]$).

Using this model, we can determine the position of the boundary of the region of Patched up-regulation (x_A), and the level of $[HH_b]$ at that position (α_A). Considering just the high Patched-producing region, Result S8(a) (with $f_p([S]) = 1$) gives the following approximation for α_A:

$$\alpha_A = \frac{(\rho_{p1} + \rho_{p2} - \gamma_p z_A)(\gamma_{ph} + k_{off})}{(\gamma_{ph} + r(\rho_{p1} + \rho_{p2}))k_{on} z_A}. \qquad \text{(Giving Eqn 13)}$$

We can then use this result to solve the steady-state equations and obtain an expression for x_A.

Assuming L_A and $k_{on}\delta$ are sufficiently large that an exponential approximation to the anterior tail gradient is appropriate, the steady state solutions are

$$[HH_b] = \begin{cases} \dfrac{\rho_{p1} + \rho_{p2}}{2D_b}x^2 + bx + c, & 0 \leq x < x_A, \\ \\ \alpha_A \exp\dfrac{(x_A - x)}{\lambda_A}, & x_A \leq x \leq L_A, \end{cases}$$

for arbitrary constants b and c and where $\lambda_A = \sqrt{\dfrac{D_b}{k_{on}\delta}}$.

Enforcing continuity of the gradient and flux when moving between regions and setting $[HH_b] = \alpha_0$ at the AP boundary ($x = 0$) gives the following conditions:

(i) $c = \alpha_0$,

(ii) $\dfrac{\rho_{p1} + \rho_{p2}}{2D_b}x_A^2 + bx_A + c = \alpha_A$,

(iii) $b = -\dfrac{\alpha_A}{\lambda_A} - \dfrac{\rho_{p1} + \rho_{p2}}{D_b}x_A$.

Substituting (i) and (iii) into (ii), and solving the quadratic, gives

$$x_A = \frac{D_b}{\rho_{p1} + \rho_{p2}}\left(\sqrt{\frac{2(\rho_{p1} + \rho_{p2})}{D_b}(\alpha_0 - \alpha_A) + \left(\frac{\alpha_A}{\lambda_A}\right)^2} - \frac{\alpha_A}{\lambda_A}\right). \qquad \text{(Giving Eqn 14)}$$

This expression can then be used to give an expression for b. Using this model, we can calculate the magnitude g of the Hedgehog gradient at the AP boundary ($x = 0$). We consider two cases, depending on whether or not the level of HH at the AP boundary is above the level required for maximal Patched up-regulation. If $\alpha_0 > \alpha_A$, the gradient at the AP boundary ($x = 0$) is equal to b. Therefore, the magnitude of the gradient is

$$g = \frac{\alpha_A}{\lambda_A} + \frac{\rho_{p1} + \rho_{p2}}{D_b} x_A = \sqrt{\frac{2(\rho_{p1} + \rho_{p2})}{D_b}(\alpha_0 - \alpha_A) + \frac{\delta k_{on} \alpha_A^2}{D_b}}. \qquad \text{(Giving Eqn 15)}$$

If $\alpha_0 \leq \alpha_A$, we ignore the first region ($x \in [0, x_A)$) and assume $x_A = 0$ and let $\alpha_A = \alpha_0$ in the equation for the second region ($x \in [x_A, L_A]$) to give an exponential gradient. Then, the gradient at the AP boundary is

$$g = \frac{\alpha_0}{\lambda_A} = \alpha_0 \sqrt{\frac{\delta k_{on}}{D_b}}. \qquad \text{(Giving Eqn 15)}$$

2 Justification of parameter constraints

Table 1 lists a number of parameter constraints and assumptions for the non-dimensionalised model, based on a number of published experimental results and model approximations (described above). Here, we justify each of the constraints C1–C10.

C1,C2: Reversible binding

The binding of HH to HSPGs and PTC is reversible, but the forward reaction is assumed to be dominant—i.e. $k_{in} \ll k_{out}$ (**C1**) and $k_{off} \ll k_{on}$ (**C2**). This is in line with the approach taken by previous models (e.g. Eldar et al. (2003), Hufnagel et al. (2006)).

C3,C4,C5: Degradation rates

Since HSPGs stabilise HH (Lin (2004), Bornemann et al. (2004)), we also assume that the degradation rate for the HH-HSPG complex is lower than those associated with other forms of PTC or HH. i.e. $\gamma_b \ll \gamma_f, \gamma_p$ and γ_{ph} (**C3**).

Experimental evidence has shown that the degradation rate of HH-PTC is faster than that of unbound PTC (Incardona et al. (2002)). Therefore, in the model $\gamma_{ph} > \gamma_p$, and in simulations we assume that $\gamma_{ph} = 6\gamma_p$ (**C4**).

Dally and Dally-like protect HH from degradation (Lin (2004), Bornemann et al. (2004)). Therefore, in the model, we assume that free HH is (relatively) unstable. In simulations we assume that $\gamma_f = 6\gamma_p \gg \gamma_b$ (**C5**).

C6: Free HH Diffusion

Dally and Dally-like are necessary for transporting HH across the disc tissue (Han et al. (2004)). Therefore, in the model, we assume that free HH diffuses slowly. i.e. $D_f \ll D_b$.

C7: PTC antagonism by HH-PTC

Experimental evidence has shown that both PTC and HH-PTC (PH) levels play important roles in Hedgehog signalling and in regulating the level of expression of target genes *col* and *dpp* (Casali and Struhl (2004)). In particular

(a) 220% HH-PTC and 80% PTC leads to target gene expression,

(b) 50% HH-PTC and 80% PTC does not lead to target gene expression,

(c) 220% HH-PTC and 140% PTC does not lead to target gene expression,

where the levels are a percentage of PTC levels at the margin ($\frac{\rho_{p1}}{\gamma_p}$ in our model). In our model, signalling activity is regulated by $[Z] = \dfrac{[PTC]}{1 + r[PH]}$, which can be rearranged to give $r = \dfrac{[PTC] - [Z]}{[PH][Z]}$. For different threshold values Z_T (scaled between 0 and 1 after non-dimensionalisation), the above data can then be substituted in to estimate reasonable values for r .

Z_T	$r_{\min}$	$r_{\max}$
0.1	3.18	5.91
0.2	1.36	2.72
0.3	0.76	1.67
0.4	0.45	1.14
0.5	0.27	0.82
0.6	0.15	0.61

From Glise et al. (2002), *col* and *dpp* are expressed in stripes of width 7 and 12 cells from the AP boundary, respectively (in 3rd instar wing discs), and so we need r to be consistent with a range of values for Z_T. A value of $r = 0.8$ is chosen to be consistent with Z-thresholds between 0.3 and 0.5 (moderate levels of signalling), where lower values of $[Z]$ correspond to high signalling.

C8: Patched up-regulation near the AP-boundary

Patched is up-regulated at the AP boundary, with total protein levels ($[PTC] + [PH]$) approximately seven times higher than at the the anterior margin, where there is virtually no signalling (Casali and Struhl (2004)). Using Result S8 (in Section 3 of this *Supporting Text*), $[PTC] + [PH] \to \dfrac{\rho_{p1} + \rho_{p2}}{\gamma_{ph}}$ as $[HH_b] \to \infty$ and $f_p([S]) \to 1$. However, $[PTC] + [PH]$ levels can be higher in other sections of the high Patched producing region (see e.g. Fig. 4A of main text). Therefore, to ensure $[PTC] + [PH] > 6\dfrac{\rho_{p1}}{\gamma_p}$ in the high Patched producing region, we let $\rho_{p2} = 6\dfrac{\gamma_{ph}\rho_{p1}}{\gamma_p}$. Simulations show that this approximation is reasonable for this model (red line in Fig. 4A of main text).

C9: Diffusion and binding rates

Patched up-regulation is evident in a band approximately five cells wide on the anterior side of the AP boundary (in 3rd instar wing discs, Glise et al. (2002)). In Model C, this corresponds to a Patched up-regulation boundary $x_A \approx 5$ cell widths. From Eqn 13 and 14

$$x_A = \frac{D_b}{\rho_{p1}+\rho_{p2}}\left(\sqrt{\frac{2(\rho_{p1}+\rho_{p2})}{D_b}(\alpha_0-\alpha_A)+\left(\frac{\alpha_A}{\lambda_A}\right)^2}-\frac{\alpha_A}{\lambda_A}\right),$$

where $\lambda_A = \sqrt{\dfrac{D_b}{\delta k_{on}}}$, $\alpha_A = \dfrac{(\rho_{p1}+\rho_{p2}-\gamma_p z_A)(\gamma_{ph}+k_{off})}{(\gamma_{ph}+r(\rho_{p1}+\rho_{p2}))k_{on}z_A}$ and δ is an approximation of $[PTC]$ and constrained by Eqn 18 (see Model C). Re-arranging the above (as shown in Result S13 in Section 3 of this *Supporting Text*) then gives

$$D_b = \left(\frac{x_A(\rho_{p1}+\rho_{p2})}{-\alpha_A\sqrt{\delta k_{on}}+\sqrt{2(\rho_{p1}+\rho_{p2})(\alpha_0-\alpha_A)+\alpha_A^2\delta k_{on}}}\right)^2.$$

From available data, we cannot yet constrain either α_0 (the level of $[HH_b]$ at the AP boundary) or z_A (the $[Z]$ threshold for Patched production). If we assume $\alpha_0 = 10$ and $z_A = 0.3$, then the non-dimensionalised model and constraints **C1**–**C8** can be used to give D_b in terms of k_{on}. Fig. ST2 (below) shows D_b as a function of k_{on} (when $\delta = 0.6$), together with the maximum signalling range for those values of D_b and k_{on}. For large k_{on}, the maximum range is less than the range of *dpp* (12–15 cells). Meanwhile, for small k_{on}, D_b and α_A become very large, implying a very shallow Hh gradient close to the source (which is not evident from experimental data such as Su et al. (2007)). For the purposes of this paper we select non-dimensionalised $k_{on} = 8$ and $D_b = 60$ in the moderate region. From *Supporting Figure* S16, we see that $\delta = 0.6$ is an appropriate value to use.

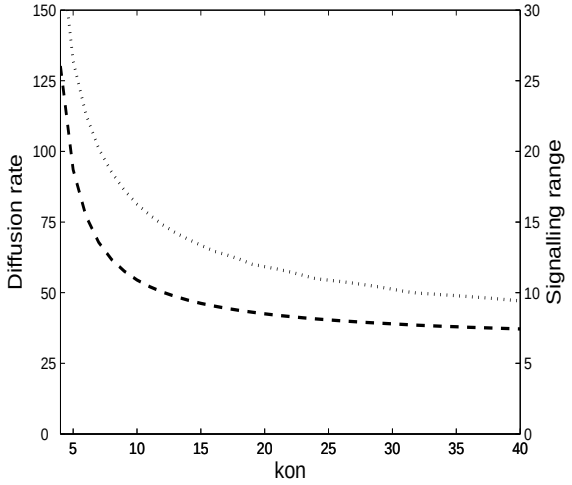

Figure ST2: Dashed line: Diffusion rate D_b in terms of k_{on} in Constraint C9 (for Model C). Dotted line: Signalling range when the model has those values D_b and k_{on}. This is defined as the position (number of cells from AP boundary) at which $[S] = 0.1$.

C10: HH levels at the AP boundary

Quantitative experimental data on the Hedgehog gradient show that the level of HH at the AP boundary is lower than that at the margin, but not by a large factor (Tabata and Takei (2004), Eugster et al. (2007)). Denoting the ratio between $[HH_b]$ at the posterior margin and the AP boundary by β, Eqn. (17) provides an approximation

$$\beta = \frac{1}{2} + \sqrt{\frac{1}{4} + \frac{\mu D_b(A)\gamma(A)}{2\rho_h D_b(P)}},$$

where $\gamma(A)$ is a generic degradation rate for HH in the anterior compartment. As with Model C, we can estimate this to be $\gamma(A) = \delta_B k_{on}$, although we note that δ_B may differ from δ in Model C.

If we further assume that D_b is uniform across the whole disc ($D_b(P) = D_b(A)$), we get

$$\rho_h = \frac{\mu \delta_B k_{on}}{2\beta\,(\beta - 1)}.$$

For the purposes of the parameter estimation, we assume $\alpha_0 = 10$ and this ratio to be approximately $\beta = 2$ (giving $\mu = \alpha_0\beta = 20$). Moreover, we have $k_{on} = 8$ (from **C9**) and assume $\delta_B = 0.75$ from numerical simulations. This then gives $\rho_h = 30$. From *Supporting Figure* S16, we can see that $\delta = 0.75$ is a suitable value to use.

3 Supplementary results and proofs

For the purposes of completeness, we provide proofs for a number of results stated in the text. These results relate to the three model approximations (A, B and C) introduced in the main text and we deal with each of these models in turn

Model A results

Result S1. *In Model A, suppose g_A and g_P are the steady state anterior and posterior gradients at the AP border. i.e. $g_i = \dfrac{d[HH]_b}{dx}$ as $x \to 0$ and $t \to \infty$, for the anterior and posterior equations.*

Then,

$$\frac{g_P}{g_A} = \frac{D_b(A)}{D_b(P)}$$

Proof:

If $D_b(P) \neq D_b(A)$, then we have a discontinuity in the gradient at the AP boundary. In this case the (transitional) diffusion term can be written as

$$D_b \frac{\partial^2 [HH_b]}{\partial x^2} = \lim_{\triangle \to 0} \frac{D_b(P)([HH_b](\triangle) - [HH_b](0)) - D_b(A)([HH_b](0) - [HH_b](-\triangle))}{\triangle^2}$$

Then, at steady state ($\frac{\partial [HH_b]}{\partial t} = 0$),

$$\begin{aligned}
\rho + \gamma[HH_b] &= \lim_{\triangle \to 0} \frac{D_b(P)([HH_b](\triangle) - [HH_b](0)) - D_b(A)([HH_b](0) - [HH_b](-\triangle))}{\triangle^2}, \\
\lim_{\triangle \to 0} \triangle(\rho + \gamma[HH_b]) &= \lim_{\triangle \to 0} \frac{D_b(P)([HH_b](\triangle) - [HH_b](0))}{\triangle} - \frac{D_b(A)([HH_b](0) - [HH_b](-\triangle))}{\triangle}, \\
0 &= D_b(P) g_P - D_b(A) g_A, \\
\frac{g_P}{g_A} &= \frac{D_b(A)}{D_b(P)}.
\end{aligned}$$

□

Result S2. *In Model A, the ratio between Hedgehog levels at the Posterior margin ($x = L_P$) and AP border ($x = 0$) is*

$$\beta = 1 + \frac{D_b(A)}{D_b(P)} \frac{\lambda_P}{\lambda_A} \left(\frac{1}{\tanh \frac{L_P}{\lambda_P}} \left(1 - \frac{1}{\cosh \frac{L_P}{\lambda_P}} \right) \right). \qquad \text{(Eqn 16)}$$

Proof:

From Model A, we can calculate the the level of HH at the Posterior margin ($x = L_P$) as

$$\begin{aligned}
[HH_b](x = L_P) &= \frac{\rho_h}{\gamma(P)} + \left(\alpha_0 - \frac{\rho_h}{\gamma(P)} \right) \cosh \frac{L_P}{\lambda_P} + \left(\alpha_0 \frac{D_b(A)}{D_b(P)} \frac{\lambda_P}{\lambda_A} \right) \sinh \frac{L_P}{\lambda_P} \\
&= \frac{\rho_h}{\gamma(P)} \left(1 - \cosh \frac{L_P}{\lambda_P} \right) + \alpha_0 \left(\cosh \frac{L_P}{\lambda_P} + \frac{D_b(A)}{D_b(P)} \frac{\lambda_P}{\lambda_A} \sinh \frac{L_P}{\lambda_P} \right).
\end{aligned}$$

Therefore

$$\beta = \frac{[HH_b](x = L_P)}{\alpha_0} = \frac{\rho_h}{\gamma(P)} \frac{1}{\alpha_0} \left(1 - \cosh \frac{L_P}{\lambda_P} \right) + \cosh \frac{L_P}{\lambda_P} + \frac{D_b(A)}{D_b(P)} \frac{\lambda_P}{\lambda_A} \sinh \frac{L_P}{\lambda_P},$$

and after substituting α_0 (from Eqn. (9) in main text) back in, we get

$$\begin{aligned}\beta &= 1 + \frac{D_b(A)}{D_b(P)}\frac{\lambda_P}{\lambda_A}\frac{1}{\tanh\dfrac{L_P}{\lambda_P}}\left(1 - \cosh\frac{L_P}{\lambda_P} + \sinh\frac{L_P}{\lambda_P}\tanh\frac{L_P}{\lambda_P}\right)\\ &= 1 + \frac{D_b(A)}{D_b(P)}\frac{\lambda_P}{\lambda_A}\frac{1}{\tanh\dfrac{L_P}{\lambda_P}}\left(1 - \frac{\cosh^2\dfrac{L_P}{\lambda_P} - \sinh^2\dfrac{L_P}{\lambda_P}}{\cosh\dfrac{L_P}{\lambda_P}}\right)\\ &= 1 + \frac{D_b(A)}{D_b(P)}\frac{\lambda_P}{\lambda_A}\left(\frac{1}{\tanh\dfrac{L_P}{\lambda_P}}\left(1 - \frac{1}{\cosh\dfrac{L_P}{\lambda_P}}\right)\right).\end{aligned}$$

□

Model B results

Result S3. *When $x_P < L_P$, in Model B, the ratio between HH levels at the Posterior margin ($x = L_P$) and AP border ($x = 0$) is*

$$\beta = \frac{1}{2} + \sqrt{\frac{1}{4} + \frac{\mu D_b(A)^2}{2\rho_h\lambda_A^2 D_b(P)}}. \qquad \text{(Eqn 17)}$$

Proof:

First, we note that $\beta = \dfrac{\mu}{\alpha_0}$. Substituting $\mu = \beta\alpha_0$ into Eqn. (10) of main text (case: $x_P < L_P$) and re-arranging, gives

$$\alpha_0 + \frac{\rho_h\lambda_A^2 D_b(P)}{D_b(A)^2} = \frac{\rho_h\lambda_A^2 D_b(P)}{D_b(A)^2}\sqrt{1 + \frac{2\alpha_0\beta D_b(A)^2}{\rho_h\lambda_A^2 D_b(P)}}.$$

Squaring both sides then gives

$$\alpha_0^2 + \frac{2\alpha_0\rho_h\lambda_A^2 D_b(P)}{D_b(A)^2} = \frac{2\alpha_0\beta\rho_h\lambda_A^2 D_b(P)}{D_b(A)^2},$$

and re-arranging gives

$$\beta = 1 + \frac{\alpha_0 D_b(A)^2}{2\rho_h\lambda_A^2 D_b(P)}.$$

Substituting Eqn. (10) back into the above then gives

$$\begin{aligned}\beta &= 1 + \frac{1}{2}\left(-1 + \sqrt{1 + \frac{2\mu D_b(A)^2}{\rho_h \lambda_A^2 D_b(P)}}\right) \\ &= \frac{1}{2} + \sqrt{\frac{1}{4} + \frac{\mu D_b(A)^2}{2\rho_h \lambda_A^2 D_b(P)}}.\end{aligned}$$

□

Result S4. *When $x_P > L_P$, in Model B, the HH concentration at the AP boundary ($x = 0$) is*

$$\alpha_0 = \frac{\rho_h \lambda_A L_P}{D_b(A)}. \qquad \text{(Eqn 10: } x_P > L_P\text{)}$$

Proof

In this case, Model B is equivalent to Model A, with $\gamma(P) = 0$. From model A and Eqn. (9)

$$\alpha_0 = \frac{\rho_h}{\gamma(P)}\left(\frac{\frac{\lambda_A}{\lambda_P}\tanh\frac{L_P}{\lambda_P}}{\frac{D_b(A)}{D_b(P)} + \frac{\lambda_A}{\lambda_P}\tanh\frac{L_P}{\lambda_P}}\right), \qquad \text{where } \lambda_i = \sqrt{\frac{D_b(i)}{\gamma(i)}}.$$

Letting $x = \dfrac{L_P}{\lambda_P}$ and noting that $\dfrac{1}{\lambda_P \gamma(P)} = \dfrac{L_P}{x D_b(P)}$, the above can then be rewritten as

$$\alpha_0 = \frac{\rho_h}{D_b(P)}\left(\frac{\frac{\lambda_A L_P}{x}\tanh x}{\frac{D_b(A)}{D_b(P)} + \frac{\lambda_A x}{L_P}\tanh x}\right).$$

Then we get the result since

$x \to 0$ as $\gamma(P) \to 0$,

$\dfrac{1}{x}\tanh x \to 1$ as $x \to 0$,

$x \tanh x \to 0$ as $x \to 0$.

□

Result S5. *When $x_P > L_P$, in Model B, the ratio between HH levels at the Posterior margin ($x = L_P$) and AP border ($x = 0$) is*

$$\beta = 1 + \frac{L_P D_b(A)}{2\lambda_A D_b(P)}.$$

Proof

In this case, Model B is equivalent to Model A, with $\gamma(P) = 0$. From model A and Result S2

$$\beta = 1 + \frac{D_b(A)}{D_b(P)} \frac{1}{\frac{\lambda_A}{\lambda_P} \tanh \frac{L_P}{\lambda_P}} \left(1 - \frac{1}{\cosh \frac{L_P}{\lambda_P}} \right), \qquad \text{where } \lambda_i = \sqrt{\frac{D_b(i)}{\gamma(i)}}.$$

Letting $x = \dfrac{L_P}{\lambda_P}$, the above can be rewritten as

$$\beta = 1 + \frac{D_b(A)}{D_b(P)} \frac{L_P}{\lambda_A} \left(\frac{\cosh x - 1}{x \sinh x} \right).$$

Then we get the result since

$x \to 0$ as $\gamma(P) \to 0$,

$\cosh x - 1 \approx \dfrac{x^2}{2}$ for small x,

$x \sinh x \approx x^2$ for small x.

□

Result S6. *In Model B, consider the the value of $[HH_b]$ at the AP boundary (α_0, Eqn 10 in main text) and the position of the target gene expression boundary (x_T, Eqn 12 in main text).*

The sensitivity coefficients (in response to ρ_h) are

Case: $x_P > L_P$

$$\frac{\partial \alpha_0}{\partial \rho_h} = \frac{\alpha_0}{\rho_h} \qquad \textit{and} \qquad \frac{\partial x_T}{\rho_h} = \frac{\lambda_A}{\rho_h}.$$

Case: $x_P < L_P$

$$\frac{\partial \alpha_0}{\partial \rho_h} = \frac{\alpha_0}{\rho_h} - \frac{\mu D_b(P) \lambda_A^2}{\alpha_0 D_b(A)^2 + \rho_h \lambda_A^2 D_b(P)} \qquad \textit{and} \qquad \frac{\partial x_T}{\rho_h} = \frac{\lambda_A}{\rho_h} - \frac{\mu D_b(P) \lambda_A^3}{\alpha_0 (\alpha_0 D_b(A)^2 + \rho_h \lambda_A^2 D_b(P))}.$$

Proof

From Eqn. (12) (in the main text), the target gene expression boundary (corresponding to a HH concentration $[HH_b]_T$) can be approximated as

$$x_T = \lambda_A \ln\left(\frac{\alpha_0}{[HH_b]_T}\right),$$

and so

(a) $$\frac{\partial x_T}{\partial \rho_h} = \frac{\lambda_A}{\alpha_0}\frac{\partial \alpha_0}{\partial \rho_h}.$$

In the case $x_P > L_P$, $\alpha_0 = \dfrac{\rho_h \lambda_A L_P}{D_b(A)}$ (from Eqn. (10) in the main text), and so

$$\frac{\partial \alpha_0}{\partial \rho_h} = \frac{\lambda_A L_P}{D_b(A)} = \frac{\alpha_0}{\rho_h},$$

as required. The result for $\dfrac{\partial x_T}{\rho_h}$ then follows from (a).

In the case $x_P < L_P$,

$$\alpha_0 = \frac{\rho_h \lambda_A^2 D_b(P)}{D_b(A)^2}\left(-1 + \sqrt{1 + \frac{2\mu D_b(A)^2}{\rho_h \lambda_A^2 D_b(P)}}\right)$$

(from Eqn. (10) in the main text), and so

$$\begin{aligned}\frac{\partial \alpha_0}{\partial \rho_h} &= \frac{\lambda_A^2 D_b(P)}{D_b(A)^2}\left(-1 + \sqrt{1 + \frac{2\mu D_b(A)^2}{\rho_h \lambda_A^2 D_b(P)}}\right) - \frac{\mu}{\rho_h}\frac{1}{\sqrt{1 + \dfrac{2\mu D_b(A)^2}{\rho_h \lambda_A^2 D_b(P)}}} \\ &= \frac{\alpha_0}{\rho_h} - \frac{\mu \rho_h D_b(P) \lambda_A^2}{\rho_h(\alpha_0 D_b(A)^2 + \rho_h \lambda_A^2 D_b(P))},\end{aligned}$$

as required. The result for $\dfrac{\partial x_T}{\rho_h}$ then follows from (a). □

Result S7. *Consider model B and the case $x_P < L_P$. Let $\rho_h' = c\rho_h$ and consider the resulting change in α_0 (to α_0'). Then*

- *if $c \geq 1$, then $\alpha_0 \leq \alpha_0' \leq \sqrt{c}\alpha_0$ and $x_T \leq x_T' \leq x_T + \lambda_A \ln \sqrt{c}$,*
- *if $c \leq 1$, then $\alpha_0 \geq \alpha_0' \geq \sqrt{c}\alpha_0$ and $x_T \geq x_T' \geq x_T + \lambda_A \ln \sqrt{c}$.*

Proof

From Eqn. (10) in main text (case: $x_P < L_P$)

$$\alpha_0 = \frac{\rho_h \lambda_A^2 D_b(P)}{D_b(A)^2}\left(-1 + \sqrt{1 + \frac{2\mu D_b(A)^2}{\rho_h \lambda_A^2 D_b(P)}}\right),$$

$$\alpha_0' = \sqrt{c}\frac{\rho_h \lambda_A^2 D_b(P)}{D_b(A)^2}\left(-\sqrt{c} + \sqrt{c + \frac{2\mu D_b(A)^2}{\rho_h \lambda_A^2 D_b(P)}}\right),$$

and so

$$\textbf{(1)}\quad \frac{\alpha_0'}{\alpha_0} = \sqrt{c}\frac{-\sqrt{c} + \sqrt{c + \dfrac{2\mu D_b(A)^2}{\rho_h \lambda_A^2 D_b(P)}}}{-1 + \sqrt{1 + \dfrac{2\mu D_b(A)^2}{\rho_h \lambda_A^2 D_b(P)}}}.$$

Now consider $y = -\sqrt{c} + \sqrt{c + a}$ where a is a positive constant. Then

$$\frac{dy}{dc} = \frac{\sqrt{c} - \sqrt{c + a}}{2\sqrt{c(c + a)}} \leq 0.$$

Therefore, using (1),

- if $c \geq 1$ then $\dfrac{\alpha_0'}{\alpha_0} \leq \sqrt{c}$,
- if $c \leq 1$ then $\dfrac{\alpha_0'}{\alpha_0} \geq \sqrt{c}$.

This combined with Eqns. (10) and (12), and the fact that $\dfrac{\partial \alpha_0}{\partial \rho_h} > 0$ and $\dfrac{\partial x_T}{\partial \rho_h} > 0$ gives the result. □

Model C results

Result S8. *Letting the anterior equations (Eqns (3)–(8) in the main text) reach steady state, we get*

(a) $[HH_b] = \dfrac{(\rho_{p1} + \rho_{p2} f_p([S]) - \gamma_p[Z])}{(\gamma_{ph} + r(\rho_{p1} + \rho_{p2} f_p([S])))k^\star[Z]}$,

(b) $[PTC] = \dfrac{\rho_{p1} + \rho_{p2} f_p([S])}{\gamma_p + \gamma_{ph} k^\star [HH_b]}$,

(c) $[PH] = \dfrac{(\rho_{p1} + \rho_{p2} f_p([S]))k^\star[HH_b]}{\gamma_p + \gamma_{ph} k^\star [HH_b]}$,

where

$$k^\star = \frac{k_{on}}{k_{off} + \gamma_{ph}} \text{ and } [Z] = \frac{[PTC]}{1 + r[PH]}.$$

Proof

First, we prove parts (b) and (c). Setting $\dfrac{\partial [PH]}{\partial t}$ to 0 (in Eqn. (6)) gives

(1) $[PH] = k^\star [HH_b][PTC]$,

(2) $k_{on}[HH_b][PTC] - k_{off}[PH] = \gamma_{ph}[PH] = \gamma_{ph} k^\star [HH_b][PTC]$,

where $k^\star = \dfrac{k_{on}}{k_{off} + \gamma_{ph}}$.

Setting $\dfrac{\partial [PTC]}{\partial t}$ to 0 (in Eqn. (5)), and using the above (2), then gives

(b) $[PTC] = \dfrac{\rho_{p1} + \rho_{p2} f_p([S])}{\gamma_p + \gamma_{ph} k^\star [HH_b]}$.

Substituting back into (1), then gives

(c) $[PH] = \dfrac{k^\star [HH_b](\rho_{p1} + \rho_{p2} f_p([S]))}{\gamma_p + \gamma_{ph} k^\star [HH_b]}$.

Since $[Z] = \dfrac{[PTC]}{1 + r[PH]}$, (b) and (c) then give

(3) $[Z] = \dfrac{\rho_{p1} + \rho_{p2} f_p([S])}{\gamma_p + k^\star [HH_b]\,(\gamma_{ph} + r(\rho_{p1} + \rho_{p2} f_p([S])))}$.

Rearranging then gives part (a).

□

Result S9. *Suppose Patched is up-regulated according to a step function f_p, where $f_p = 0$ (or 1) if $[Z] > z_A$ ($[Z] < z_A$). Then, at steady state, $[PTC]$ is bounded above and below by*

$$[PTC]_{max} = \frac{z_A(\gamma_{ph} + r(\rho_{p1} + \rho_{p2}))}{\gamma_{ph} + r\gamma_p z_A}$$

$$[PTC]_{min} = \frac{z_A(\gamma_{ph} + r\rho_{p1})}{\gamma_{ph} + r\gamma_p z_A} \qquad \textit{(away from the AP border).}$$

Proof:

First, let $k^\star = \dfrac{k_{on}}{\gamma_{ph} + k_{off}}$. Then, from the steady state equations, we get

(1) $[PH] = k^\star [PTC][HH_b]$

(see proof of Result S8). Then, since $[Z] = \dfrac{[PTC]}{1 + r[PH]}$, we can use (1) to get

(2) $[PTC] = \dfrac{[Z]}{1 - rk^\star [HH_b][Z]}$.

Moreover, substituting in Result S8(a), we get

(3) $[PTC] = \dfrac{[Z](\gamma_{ph} + r(\rho_{p1} + \rho_{p2} f_p))}{\gamma_{ph} + r\gamma_p [Z]}$.

Now, since we have a step function f_p, we have the following three scenarios

(a) $[Z] < z_A$ and $[PTC] = \dfrac{\rho_{p1} + \rho_{p2}}{\gamma_p + \gamma_{ph} k^\star [HH_b]}$ (from Result S8(b) with $f_p = 1$)

(b) $[Z] = z_A$ and $[PTC] = \dfrac{z_A}{1 - rk^\star [HH_b] z_A}$ (from (2))

(c) $[Z] > z_A$ and $[PTC] = \dfrac{\rho_{p1}}{\gamma_p + \gamma_{ph} k^\star [HH_b]}$ (from Result S8(b) with $f_p = 0$).

Therefore, we have

(a) $\dfrac{\partial[PTC]}{\partial[HH_b]} < 0,$

(b) $\dfrac{\partial[PTC]}{\partial[HH_b]} > 0,$

(c) $\dfrac{\partial[PTC]}{\partial[HH_b]} < 0.$

Therefore, away from the AP border (where PTC may be completely saturated by HH) the maximum and minimum for Patched occurs as $[Z] \to z_A$ in the cases (a) and (c) respectively. Therefore, we get $[PTC]_{max}$ ($[PTC]_{min}$) by letting $[Z] = z_A$ and $f_p = 1(0)$ in (3) above.

□

Result S10. *Suppose k_{off} is relatively small, so that we can choose δ satisfying*

$$\delta \leq \frac{z_A(\gamma_{ph} + r(\rho_{p1} + \rho_{p2}))}{\gamma_{ph} + r\gamma_p z_A + k_{off}}\ , \qquad \delta \leq [PTC]_{max},$$
$$\delta \geq [PTC]_{min},$$

where $[PTC]_{min}$ and $[PTC]_{max}$ are as defined in Result S9. Then we get

$$((\rho_{p1} + \rho_{p2}) - \alpha_A \delta k_{on}) \geq 0,$$

where $\alpha_A = \dfrac{(\rho_{p1} + \rho_{p2} - \gamma_p z_A)(\gamma_{ph} + k_{off})}{(\gamma_{ph} + r(\rho_{p1} + \rho_{p2}))k_{on} z_A}$ *(as defined in Eqn. (13) in the main text).*

Proof:

From Eqn. (13) (main text)

$$\alpha_A = \frac{(\rho_{p1} + \rho_{p2} - \gamma_p z_A)(\gamma_{ph} + k_{off})}{(\gamma_{ph} + r(\rho_{p1} + \rho_{p2}))k_{on} z_A}$$

is defined as the level of $[HH_b]$ when $[Z] = z_A$ in the high Patched production region. Therefore,

$$\begin{aligned}
\alpha_A \delta k_{on} &\leq k_{on} \frac{(\rho_{p1} + \rho_{p2} - \gamma_p z_A)(\gamma_{ph} + k_{off})}{(\gamma_{ph} + r(\rho_{p1} + \rho_{p2}))k_{on} z_A} \frac{z_A(\gamma_{ph} + r(\rho_{p1} + \rho_{p2}))}{\gamma_{ph} + r\gamma_p z_A + k_{off}} \\
&\leq \frac{((\rho_{p1} + \rho_{p2}) - \gamma_p z_A)(\gamma_{ph} + k_{off})}{\gamma_{ph} + r\gamma_p z_A + k_{off}} \\
&\leq (\rho_{p1} + \rho_{p2}) - \gamma_p z_A \\
&\leq (\rho_{p1} + \rho_{p2}).
\end{aligned}$$

□

Result S11. *In Model C, consider x_A from Eqn 14 (main text). If we assume that δ is bounded by the conditions in Result S10, then*

(a) $\dfrac{\partial x_A}{\partial r} > 0$,

(b) $\dfrac{\partial x_A}{\partial k_{on}} > 0$.

Proof

First, we show $\dfrac{\partial x_A}{\partial \alpha_A} < 0$. Then since $\dfrac{\partial \alpha_A}{\partial r} < 0$ and $\dfrac{\partial \alpha_A}{\partial k_{on}} < 0$ (from Eqn 13), we get the result.

Differentiating x_A (Eqn 14) with respect to α_A and noting that $\lambda_A = \sqrt{\dfrac{D_b}{\delta k_{on}}}$, we get

$$\begin{aligned}\frac{\partial x_A}{\partial \alpha_A} &= \frac{D_b}{2(\rho_{p1}+\rho_{p2})\sqrt{\left(\dfrac{\alpha_A}{\lambda_A}\right)^2 + \dfrac{2(\rho_{p1}+\rho_{p2})}{D_b}(\alpha_0-\alpha_A)}}\left(-\frac{2(\rho_{p1}+\rho_{p2})}{D_b} + \frac{2\alpha_A}{\lambda_A^2}\right) - \frac{D_b}{(\rho_{p1}+\rho_{p2})\lambda_A} \\ &< \frac{D_b}{(\rho_{p1}+\rho_{p2})\sqrt{\left(\dfrac{\alpha_A}{\lambda_A}\right)^2 + \dfrac{2(\rho_{p1}+\rho_{p2})}{D_b}(\alpha_0-\alpha_A)}}\left(-\frac{(\rho_{p1}+\rho_{p2}) + \alpha_A\delta k_{on}}{D_b}\right).\end{aligned}$$

Then, since $((\rho_{p1}+\rho_{p2}) - \alpha_A\delta k_{on}) \geq 0$ from Result S10, we get $\dfrac{\partial x_A}{\partial \alpha_A} < 0$.

□

Result S12. *Suppose δ is bounded by the conditions in Result S10. Then, the gradient at the AP border increases (or remains unchanged) in any of the following circumstances:*

1. *α_A decreases due to a single parameter change (excluding p_{p1} or p_{p2}),*
2. *D_b decreases,*
3. *α_0 increases.*

Proof

From Eqn. (15) (main text), this absolute gradient can be approximated by

Case A. $\alpha_0 \geq \alpha_A$

$$g_A = \sqrt{\frac{2(\rho_{p1}+\rho_{p2})}{D_b}(\alpha_0 - \alpha_A) + \frac{\delta k_{on}\alpha_A^2}{D_b}}.$$

Case B. $\alpha_0 < \alpha_A$

$$g_B = \alpha_0\sqrt{\frac{\delta k_{on}}{D_b}},$$

where $\alpha_A = \dfrac{(\rho_{p1}+\rho_{p2}-\gamma_p z_A)(\gamma_{ph}+k_{off})}{(\gamma_{ph}+r(\rho_{p1}+\rho_{p2}))k_{on}z_A}$ is the HH concentration threshold, above which Patched is highly up-regulated.

In both cases A and B, it is clear that $\dfrac{\partial g}{\partial D_b} \leq 0$ and $\dfrac{\partial g}{\partial \alpha_0} \geq 0$. Then, since $g_A = g_B$, when $\alpha_A = \alpha_0$, 2 and 3 must be true.

Therefore, we just need to prove the first case. We assume that $\rho_{p1}+\rho_{p2}$ and δ remain unchanged, and consider the following two cases.

1a: k_{on} increases (leading to a decrease in α_A),

1b: α_A decreases independently of $k_{on}, \rho_{p1}+\rho_{p2}$.

In case 1a,

$$\frac{dg_A}{dk_{on}} = \frac{1}{2D_b\sqrt{\dfrac{2(\rho_{p1}+\rho_{p2})}{D_b}(\alpha_0-\alpha_A)+\dfrac{\delta k_{on}\alpha_A^2}{D_b}}}\left(\delta\alpha_A^2 - 2\frac{d\alpha_A}{dk_{on}}\left((\rho_{p1}+\rho_{p2}) - \alpha_A\delta k_{on}\right)\right).$$

Then since, $\dfrac{d\alpha_A}{dk_{on}} \leq 0$ and $((\rho_{p1}+\rho_{p2}) - \alpha_A\delta k_{on}) \geq 0$ (from Result S10), we get $\dfrac{dg_A}{dk_{on}} \geq 0$. Moreover, $\dfrac{dg_B}{dk_{on}} = \alpha_0\dfrac{\sqrt{\delta}}{2\sqrt{D_b k_{on}}} \geq 0$ and so we get the desired result.

In case 1b,

$$\frac{dg_A}{d\alpha_A} = \frac{1}{2D_b\sqrt{\frac{2(\rho_{p1}+\rho_{p2})}{D_b}(\alpha_0-\alpha_A)+\frac{\delta k_{on}\alpha_A^2}{D_b}}}\left(-2\left((\rho_{p1}+\rho_{p2})-\alpha_A\delta k_{on}\right)\right).$$

Then since $((\rho_{p1}+\rho_{p2})-\alpha_A\delta k_{on}) \geq 0$ (from Result S10), we get $\frac{dg_A}{d\alpha_A} \leq 0$. Moreover, $\frac{dg_B}{\alpha_A} = 0$ in this case and so we get the desired result.

□

Result S13. *In Model C,*

$$D_b = \left(\frac{x_A(\rho_{p1}+\rho_{p2})}{-\alpha_A\sqrt{\delta k_{on}}+\sqrt{2(\rho_{p1}+\rho_{p2})(\alpha_0-\alpha_A)+\alpha_A^2\delta k_{on}}}\right)^2.$$

Proof

From Eqn. (14) (main text)

$$x_A = \frac{D_b}{\rho_{p1}+\rho_{p2}}\left(-\frac{\alpha_A}{\lambda_A}+\sqrt{\frac{2(\rho_{p1}+\rho_{p2})}{D_b}(\alpha_0-\alpha_A)+\left(\frac{\alpha_A}{\lambda_A}\right)^2}\right),$$

where

- $\lambda_A = \sqrt{\frac{D_b}{\delta k_{on}}}$,
- $\alpha_A = \frac{(\rho_{p1}+\rho_{p2}-\gamma_p z_A)(\gamma_{ph}+k_{off})}{(\gamma_{ph}+r(\rho_{p1}+\rho_{p2}))k_{on}z_A}$.

Therefore

$$\begin{aligned} x_A(\rho_{p1}+\rho_{p2}) &= D_b\left(-\frac{\alpha_A\sqrt{\delta k_{on}}}{\sqrt{D_b}}+\sqrt{\frac{2(\rho_{p1}+\rho_{p2})}{D_b}(\alpha_0-\alpha_A)+\frac{\alpha_A^2\delta k_{on}}{D_b}}\right) \\ &= \sqrt{D_b}\left(-\alpha_A\sqrt{\delta k_{on}}+\sqrt{2(\rho_{p1}+\rho_{p2})(\alpha_0-\alpha_A)+\alpha_A^2\delta k_{on}}\right). \end{aligned}$$

Squaring both sides and rearranging then gives the result. □

References

Bornemann, D., Duncan, J., Staatz, W., Selleck, S., Warrior, R., 2004. Abrogation of heparan sulfate synthesis in *drosophila* disrupts the wingless, hedgehog and decapentaplegic signaling pathways. Development 131, 1927–1938.

Casali, A., Struhl, G., 2004. Reading the hedgehog morphogen gradient by measuring the ratio of bound to unbound patched protein. Nature 431, 76–80.

Eldar, A., Rosin, D., Shilo, B., Barkai, N., 2003. Self-enhanced ligand degradation underlies robustness of morphogen gradients. Dev. Cell 5, 635–646.

Eugster, C., Pánaková, D., Mahmoud, A., Eaton, S., 2007. Lipoprotein-heparan sulfate interactions in the hh pathway. Dev. Cell 13, 57–71.

Glise, B., Jones, D., Ingham, P., 2002. Notch and wingless modulate the response of cells to hedgehog signalling in the drosophila wing. Dev. Biol. 248, 93–106.

Han, C., Belenkaya, T., Wang, B., Lin, X., 2004. *Drosophila* glypicans control the cell-to-cell movement of hedgehog by a dynamin-independent process. Development 131, 601–611.

Hufnagel, L., Kreuger, J., Cohen, S. M., Shraiman, B. I., 2006. On the role of glypicans in the process of morphogen gradient formation. Dev. Biol. 300, 512–522.

Incardona, J., Gruenberg, J., Roelink, H., 2002. Sonic hedgehog induces the segregation of Patched and Smoothened in endosomes. Curr. Biol. 12, 983–995.

Lin, X., 2004. Functions of heparan sulfate proteoglycans in cell signaling during development. Development 131, 6009–6021.

Su, V., Jones, K., Brodsky, M., The, I., 2007. Quantitative analysis of hedgehog gradient formation using an inducible expression system. BMC Dev. Biol. 7, 43.

Tabata, T., Takei, Y., 2004. Morphogens, their identification and regulation. Development 131, 703–712.

Supplementary figures

Parameter sets

This section presents a number of addition figures to supplement those in the main text. In the figures below (S1-2;S5-13) we consider 4 different parameter sets. Default parameters are taken from Table 1 (of main text) but differ as follows

Green: $r = 0$, $\rho_{p2} = 0$

Blue: $r = 0$, $\rho_{p2} = 36$

Red: $r = 0.8$, $\rho_{p2} = 36$

Black Dashed: $r = 0$, $\rho_{p2} = 36$ and k_{on} increases up to 5-fold in response to high Hh signalling (see *Materials and Methods* in main text)

FigS1: Anterior concentration profiles

These figures show HH, Total PTC ($[PTC] + [PH]$), S and Target gene levels across the anterior compartment, when we fix HH levels at the AP boundary (α_0). We have matched the four models in four different ways (A-D)

(A) Models are matched so that HH levels match at the AP boundary.

(B,C) Models are matched so that HH levels match at both the AP boundary and 12 cells from the boundary. This is done by changing ρ_{p1} in the green model and (B) k_{on} in the blue model; (C) k_{on} in the red and black dashed model.

(D) Models are matched so that the magnitude of the HH gradient is equal at the AP boundary. This is done by changing ρ_{p1} in the green model and k_{on} in the blue model.

The four different parameter sets (green, blue, red and blacked dashed) are described at the start of this supporting file.

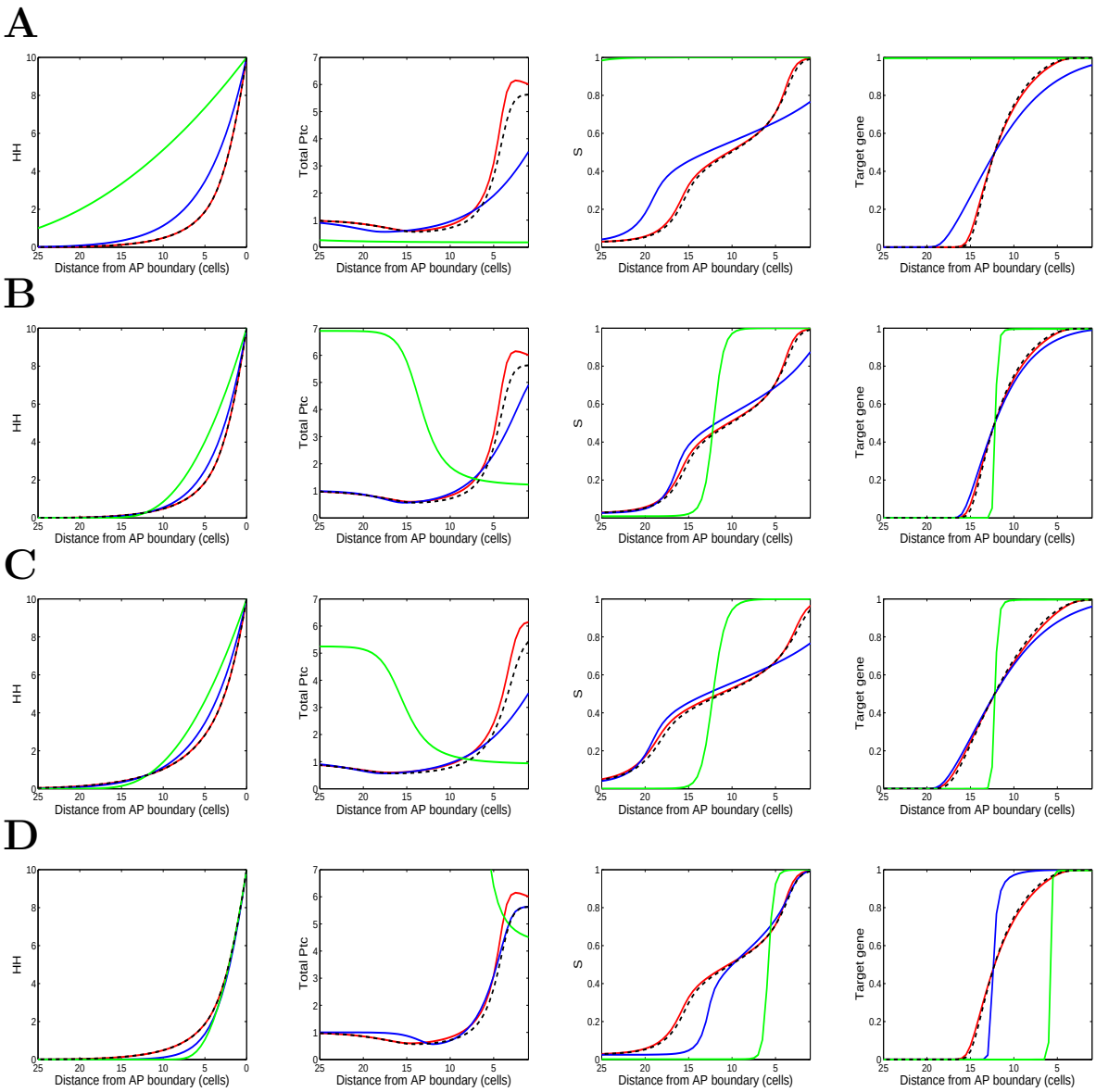

Figure S1: Anterior concentration profiles for the four models and four cases (A-D) described above.

FigS2: Posterior-Anterior concentration profiles

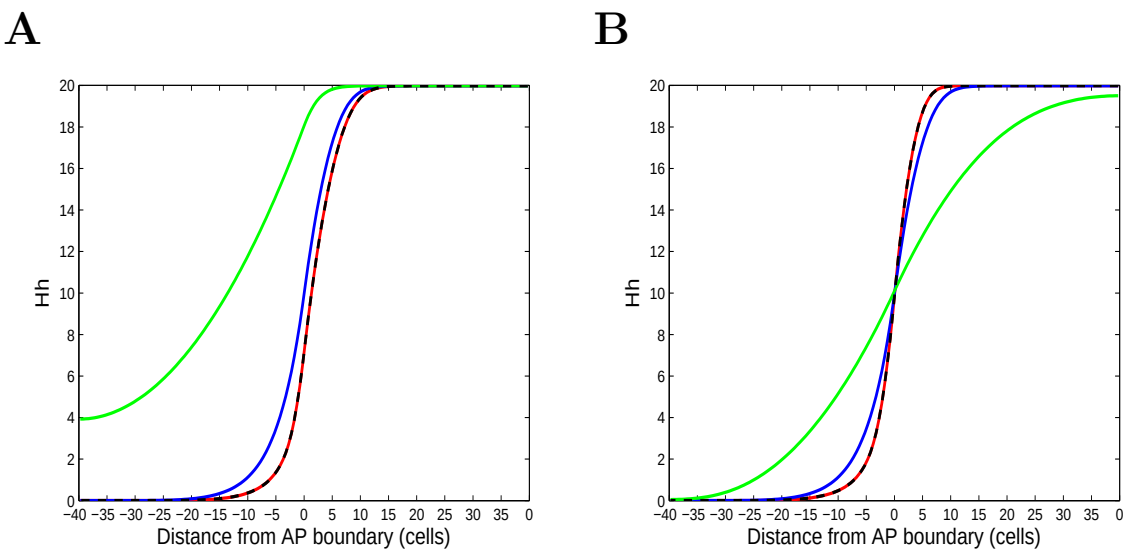

Figure S2: HH levels across a 1D cross section of disc for the full anterior-posterior model (posterior right, anterior left).(A) Models are matched so that Hedgehog production is equal ($\rho_h = 15$). (B) Hedgehog production is altered in each model to ensure HH levels are equal at the AP boundary ($\alpha_0 = 10$). $\rho_h = 30$ (red, black dashed), 15 (blue) and 1.5 (green). Otherwise, the four different parameter sets (green, blue, red and blacked dashed) are as described at the start of this supporting file.

FigS3 and FigS4: Shift in target gene boundaries for different parameter sets

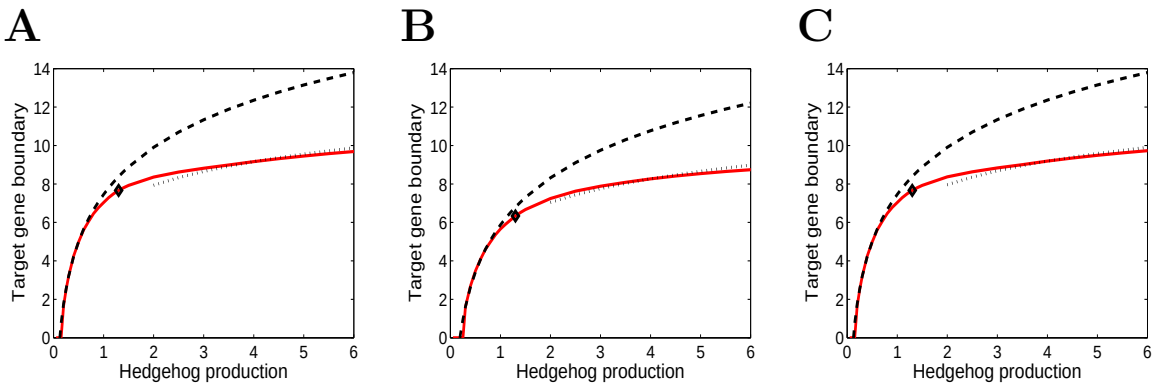

Figure S3: Shift in target gene boundary in response to changes in Hedgehog production (red). Black dashed lines correspond to theoretical predictions for free diffusion scenario, whilst dotted line corresponds to outer bound in regulated transport case ($\sqrt{c}$ case in Fig 5A of main text). Diamond corresponds to threshold ($x_P = L_P$) separating the two behaviours. In all cases parameters are taken from Table 1 but differ in the following way (A) $k_{out} = 10$, $\gamma_f = 6$ and $D_f = 0.6$. (B) $k_{out} = 2.5$ and $\gamma_f = 24$ and $D_f = 0.6$. (C) $k_{out} = 10$, $\gamma_f = 6$ and $D_f = 60$.

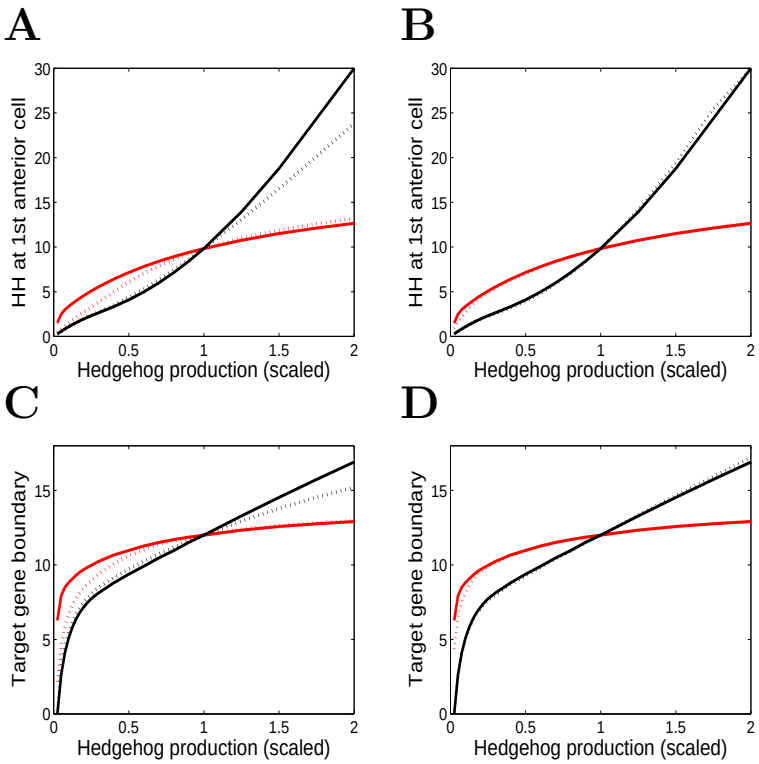

Figure S4: Shift in (A,B) HH levels at AP boundary and (C,D) target gene boundary in response to changes in Hedgehog production, for different modes of HH-HSPG interactions (achieved by varying μ, γ_b and $D_b(P)$ in the model). In all figures red and black lines differ because of the saturation parameter μ: red $\mu = 20$ vs black $\mu = 2000$. (A,C) Effect of changing the HH-HSPG degradation rate γ_b: solid line $\gamma_b = 0.01$ vs dotted line $\gamma_b = 1$. (B,D) Effect of changing the HH-HSPG diffusion rate of$D_b(P)$: solid line $D_b(P) = 60$ vs dotted line $D_b(P) = 120$. All other parameters are from Table 1 of main text.

FigS5: Robustness to changes in HH levels at the AP boundary

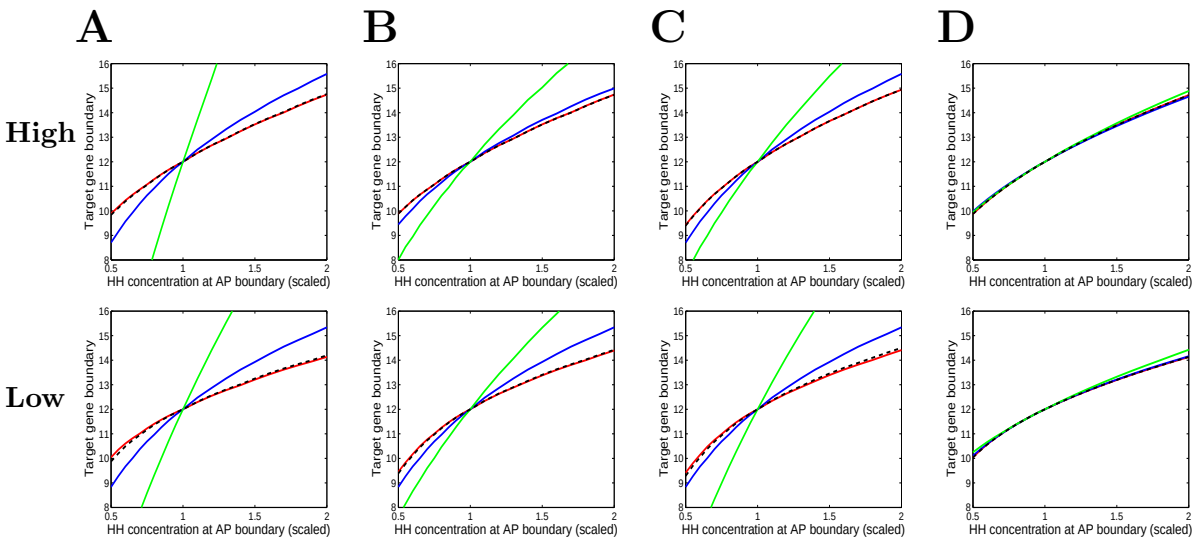

Figure S5: Shift in target gene boundary in response to changes in HH levels at the AP boundary (α_0), for the different parameter sets (green, blue, red and blacked dashed) described at the start of this supporting file. Top (High): The base levels of α_0 are taken from FigS1 (A-D) (scaled to 1 on x axis). Bottom (Low): Same but with a base levels of α_0 halved. In all cases, the HH concentration at 12 cells (when α_0 is at its base value) is used to define the target gene boundary.

FigS6: Robustness to changes in HH production in the full Posterior-Anterior model

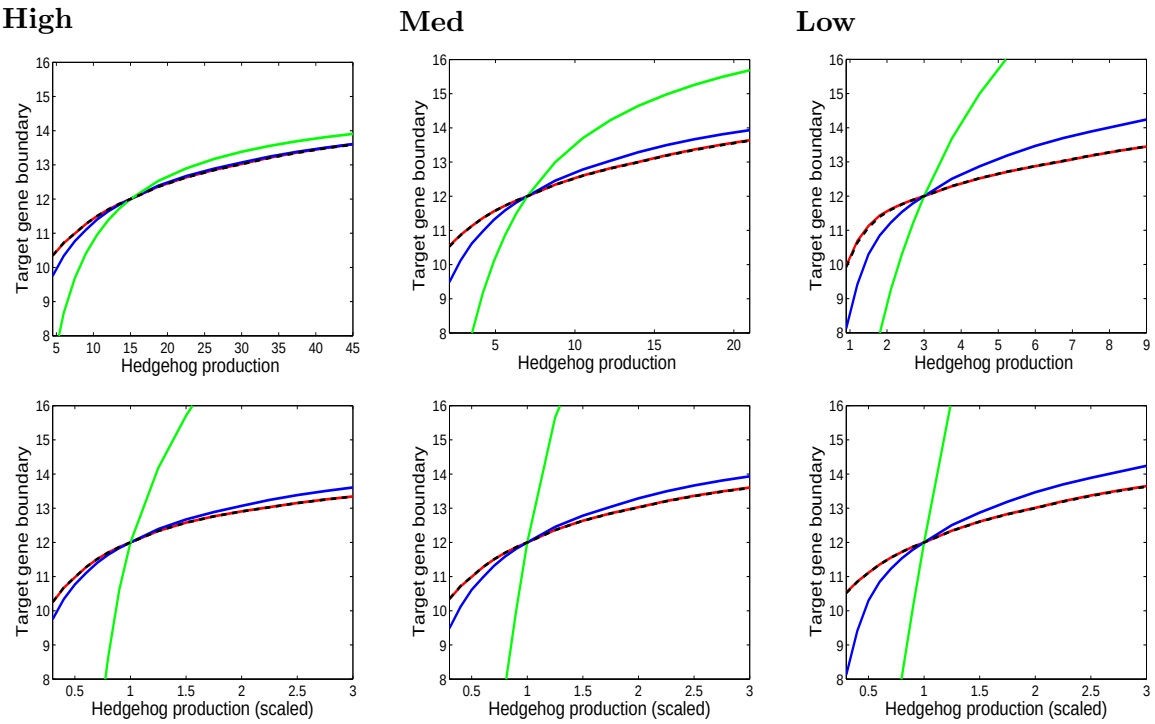

Figure S6: Shift in target gene boundary, in response to changes in Hedgehog production ρ_h, for the different parameter sets (green, blue, red and blacked dashed) described at the start of this supporting file. Top: Production rate is the same in each model (as in *Supporting Figure* S2A). Bottom: Base production rate (scaled to 1) varies in each model to ensure they match at the AP boundary (as in *Supporting Figure* S2B). These base production rates are as follows. High: red and black dashed = 30, blue = 15, green = 1.5. Med: red and black dashed = 15, blue = 7, green = 1.15. Low: red and black dashed = 7.5, blue = 3, green = 0.86. In all cases, the HH concentration at 12 cells (when ρ_h is at its base value) is used to define the target gene boundary.

FigS7 and FigS8: Robustness to changes in parameters

Shift in target gene boundary in response to parameter changes. Here, we use the full anterior-posterior model, along with the parameter sets (green, blue, red and blacked dashed) described at the start of this supporting file. In addition, the black dotted line corresponds to the case where $r = 0.4$ and k_{on} is increased 3.6-fold in response to signalling (mix of red and black dashed case). Target gene boundaries correspond to the HH concentration at 12 cells, when the parameter in question is at its default value (in Table 1) and ρ_h is its base value (from *Supporting Figure* S2B). Parameters are varied in the anterior and posterior compartments independently (Fig S7 and Fig S8 respectively)

Anterior parameters

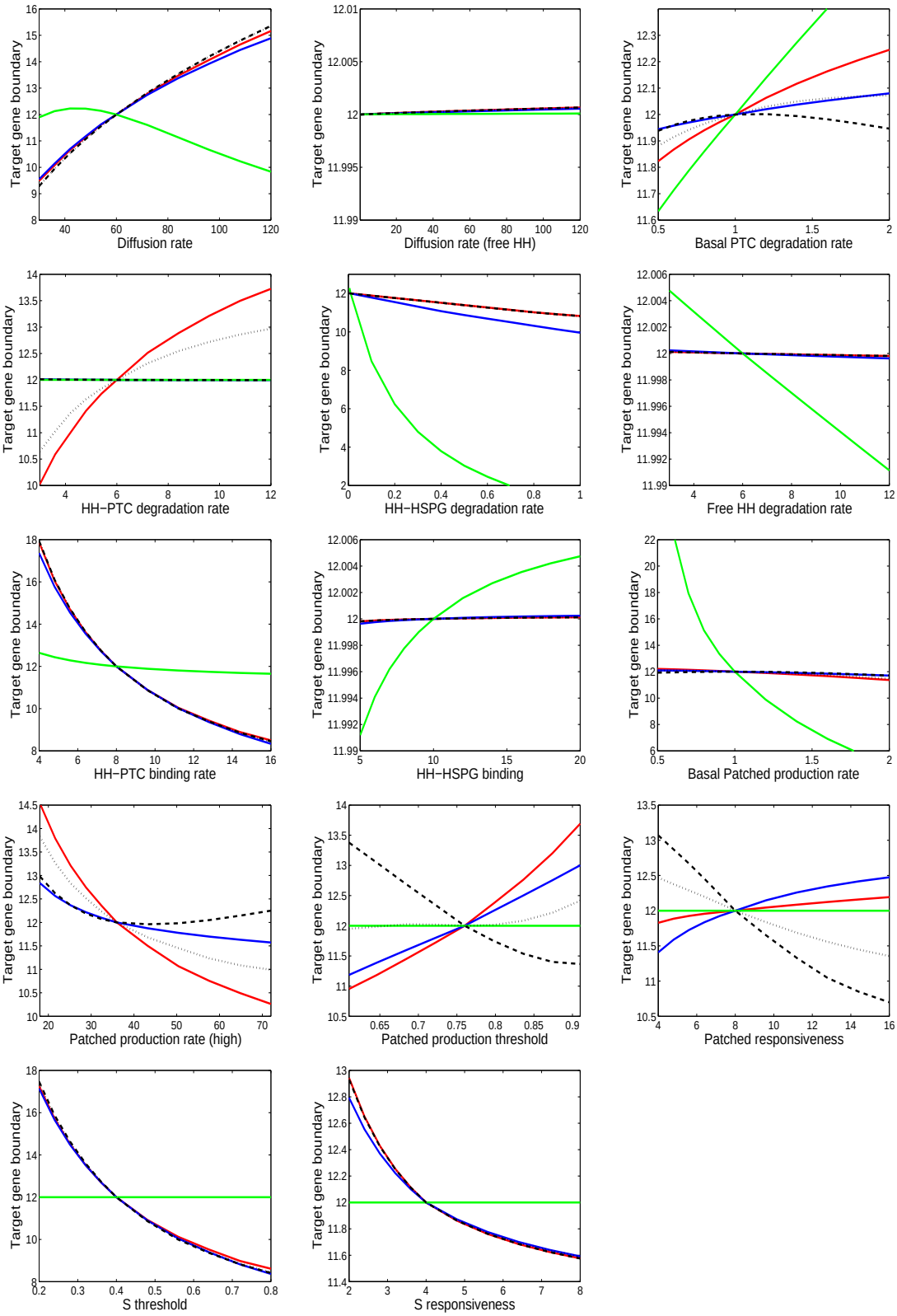

Figure S7: Shift in target gene boundary, in response to anterior parameter changes. Top: $D_b(A)$, D_f, γ_p. 2nd row: γ_{ph}, γ_b, γ_f. 3rd row: k_{on}, k_{out}, ρ_{p1}. 4th row: ρ_{p2}, c_p, n_p. 5th row: c_s, n_s. In all cases, the HH concentration at 12 cells (when parameter is at its base level) is used to define the target gene boundary.

Posterior parameters

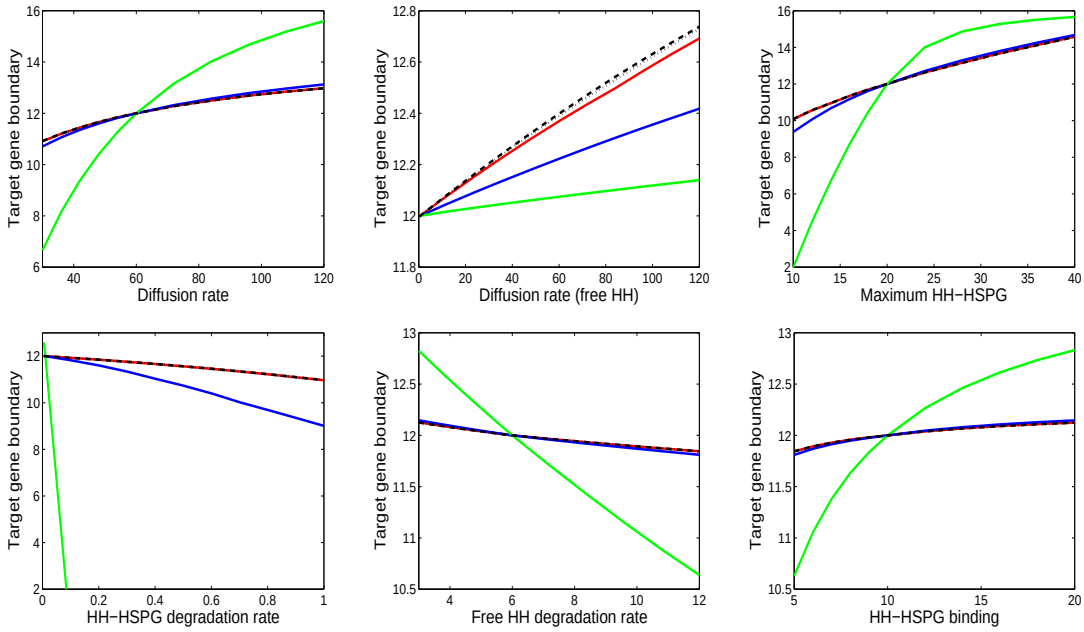

Figure S8: Shift in target gene boundary, in response to posterior parameter changes. Top: $D_b(P)$, D_f, μ. 2nd row: γ_b, γ_f, k_{out}. In all cases, the HH concentration at 12 cells (when parameter is at its base level) is used to define the target gene boundary.

FigS9: Changes in target gene expression to increases in HH

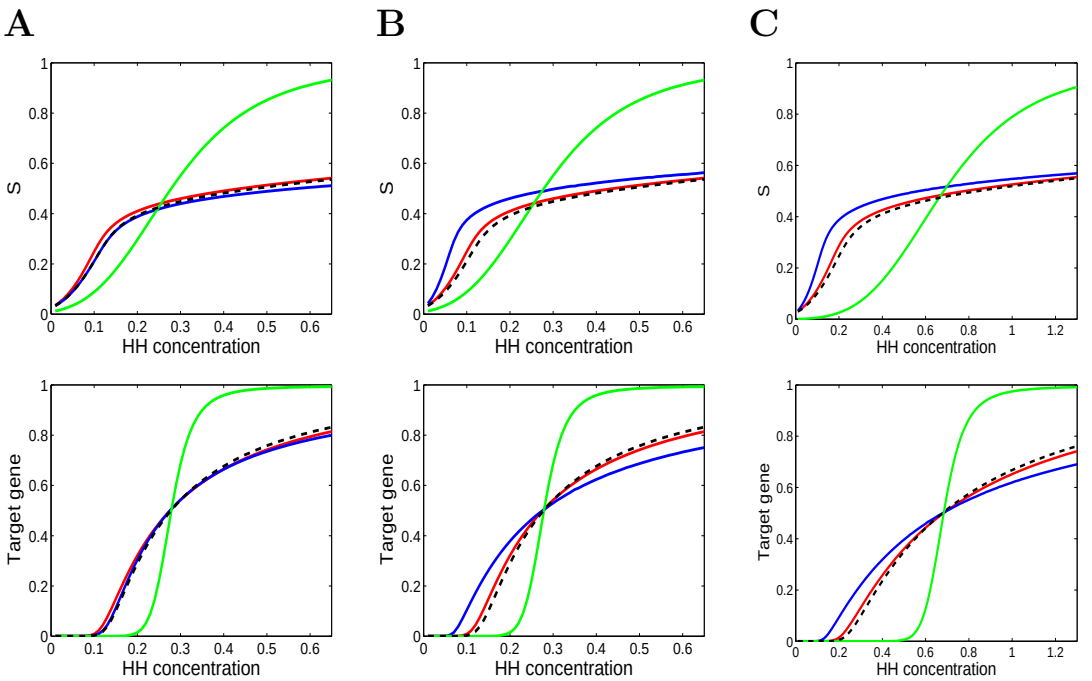

Figure S9: S and target gene response for changing HH levels. In each figure we use parameters and thresholds from A-C of *Supporting Figure* S1.

FigS10-S11: Supplementary figures for the case $n_p = 4$

In the main simulations, Patched is up-regulated according to a non-linear hill function $f = \frac{[S]^n}{[S]^n + c^n}$ where c is signalling threshold, for the response, and n is sharpness of that response. In the main text and above figures, we used a relatively high $n = 8$ since it gave a better fit with experimental data and allowed Patched production to reach a maximum (given that c is relatively large also). Here, we have repeated some of the simulations for the more conservative case $n = 4$.

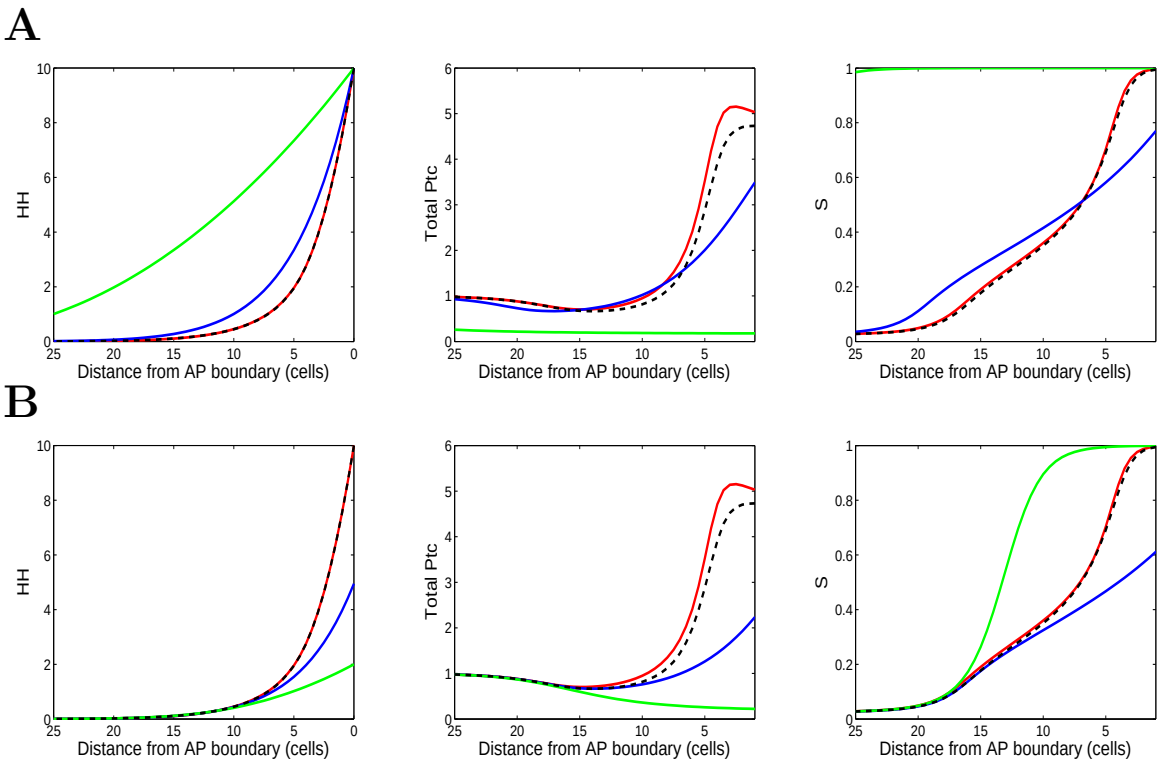

Figure S10: Repeat of Fig4 for the case $n_p = 4$

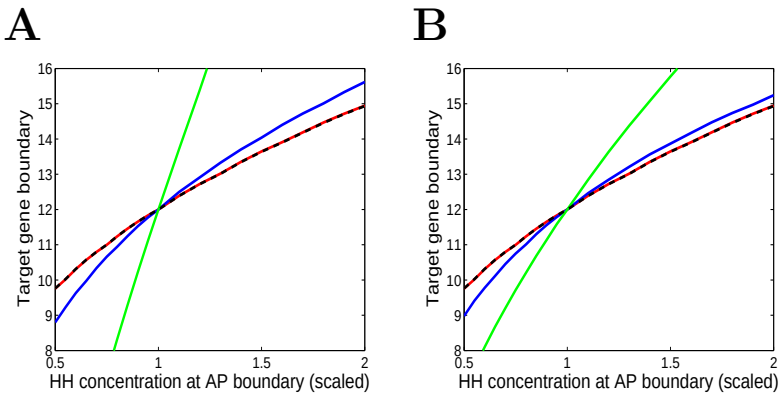

Figure S11: Repeat of Fig6A,B for the case $n_p = 4$

FigS12-S13: Supplementary figures for linear functions

In the main simulations, PTC and S are up-regulated according non-linear hill functions. However, for comparison we have also repeated some of the simulations for the case where these functions are linear. i.e. $f = \frac{[S]}{2c}$ and $g = 1 - \frac{[Z]}{2c}$ where c is the threshold corresponding to 50% response and $[S]$ and $[Z]$ are scaled between 0 and 1.

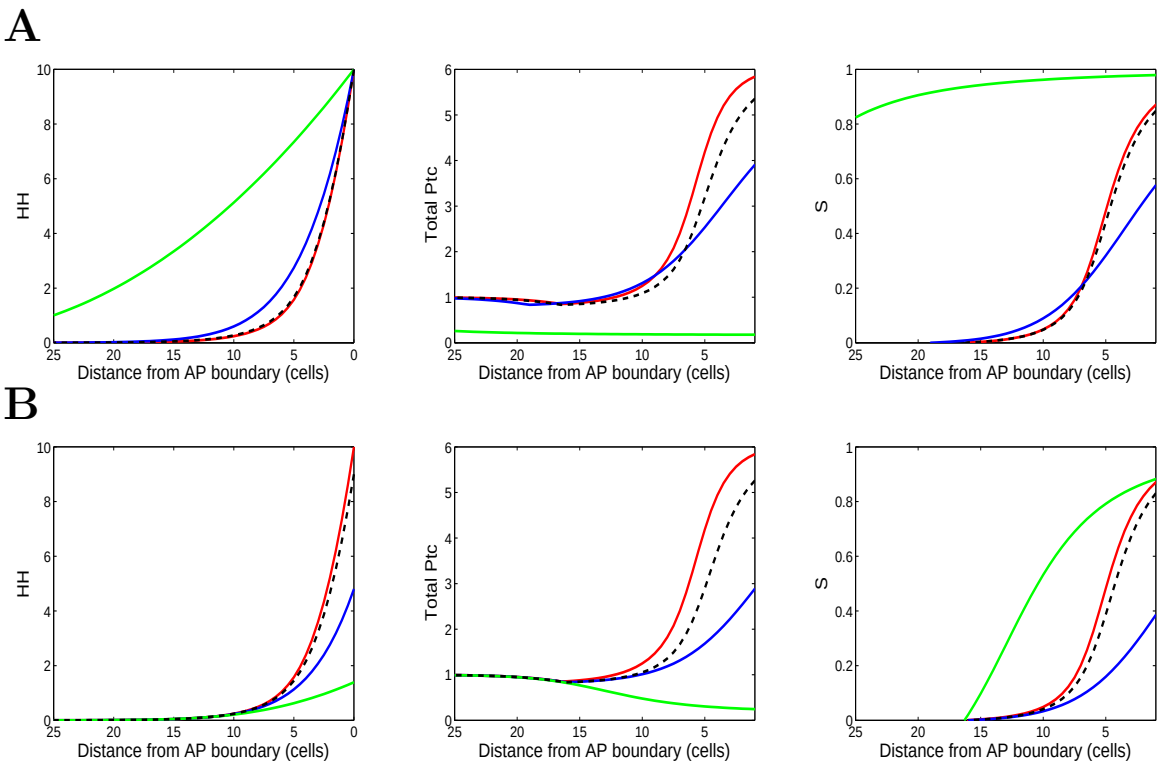

Figure S12: Repeat of Fig4 for the case of linear functions

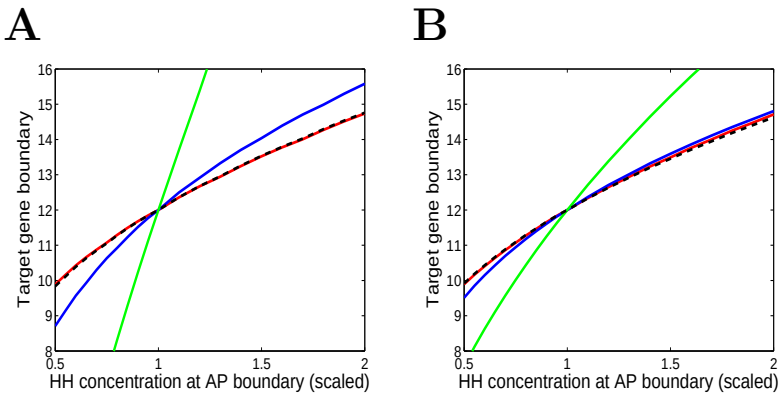

Figure S13: Repeat of Fig6A,B for the case of linear functions

FigS14-S15: Supplementary figures for alternative positive feedback

In the main model and simulations, the model considers two cases where a negative and positive feedback combine to regulate Hedgehog signalling (red and black dashed lines in Fig 4 and 6). Here, we repeat those simulations, but for an alternative positive feedback (new black dashed line in the Fig. S14 and S15).

Data suggests that an additional positive feedback loop exists between SMO and FU within the signalling pathway, which is functional in response to high levels of signalling. We therefore incorporate this feedback into the model to demonstrate that it has a qualitatively similar function to those already discussed in the main text. In order to incorporate this in the model, we altered the signalling input $[Z]$ to

$$[Z] = \frac{g_z([S])[PTC]}{1 + r[PH]}$$

where $g_z([S])$ is a decreasing (Hill) function analogous to those used in the main model. Although we don't explicitly add FU and SMO to the model, incorporating the extra interaction in this way ensures that it functions in line with the available experimental data (Claret et al. (2007), Liu et al. (2007))

(a) The positive feedback is dependent on signalling. i.e. The positive feedback can't sustain a cellular response, following transient Hedgehog exposure

(b) The positive feedback (FU, in particular) disables the ability of Patched to inhibit signalling.

Other ways of incorporating positive feedback still result in qualitatively similar results (results not shown).

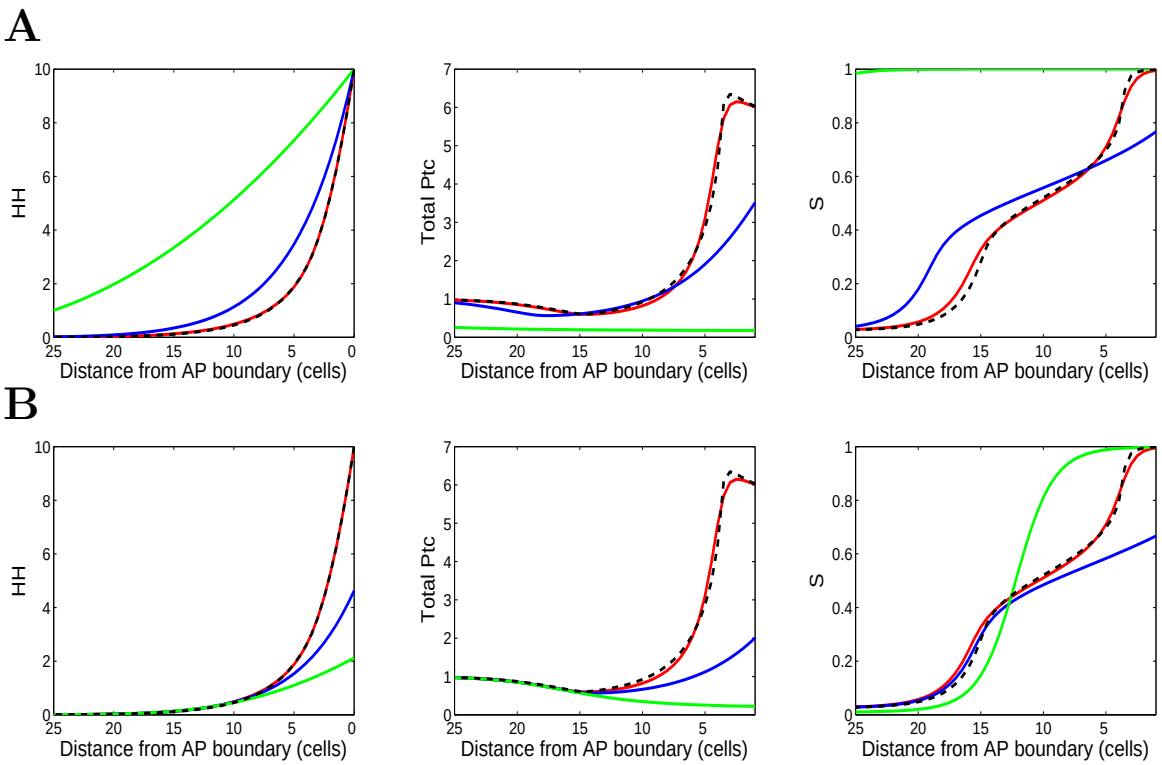

Figure S14: Repeat of Fig4 for the case when the positive feedback loop between SMO and FU is included in the model, alongside the negative feedback up-regulating Patched (Black dashed). Green, Blue, Red are as before.

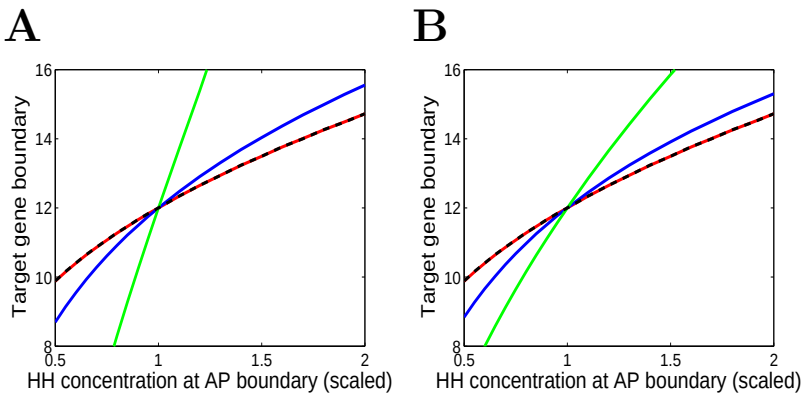

Figure S15: Repeat of Fig6A,B for the case when the positive feedback loop between SMO and FU is included in the model, alongside the negative feedback up-regulating Patched (Black dashed). Green, Blue, Red are as before.

FigS16: Model Approximations compared to full model

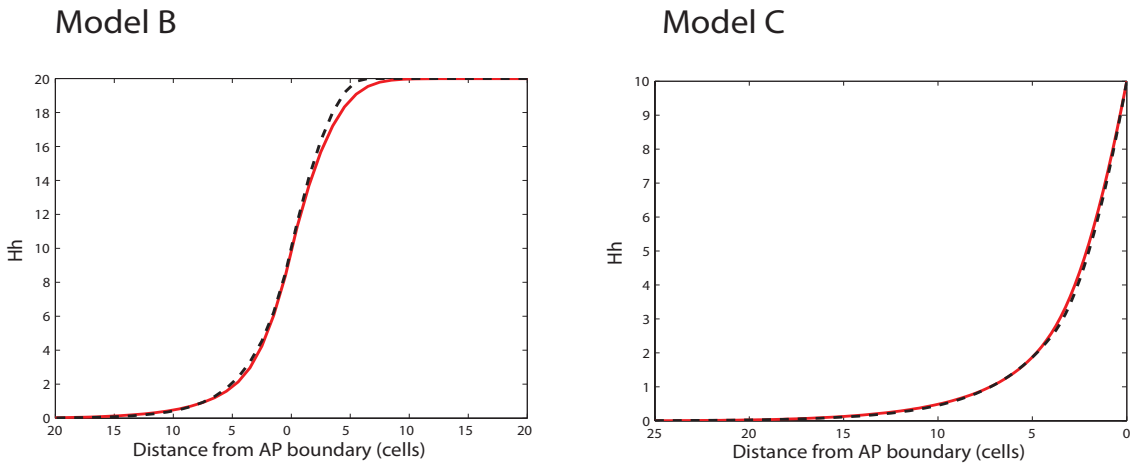

Figure S16: Model B and C approximations (dashed line) to the full model (red line), with $\gamma(A) = 0.75k_{on}$ and $\delta k_{on} = 0.6k_{on}$ respectively. The remaining parameters are those in Table 1 of main text.

Bibliography

Claret, S., Sanial, M., Plessis, A., 2007. Evidence of a novel feedback loop in the hedgehog pathway involving smoothened and fused. Curr. Biol. 17, 1326–1333.

Liu, Y., Cao, X., Jiang, J., Jia, J., 2007. Fused-costal2 protein complex regulates hedgehog-induced smo phosphorylation and cell-surface accumulation. Genes & Dev 21, 1949–1963.